Syntheses, Crystal Structures, and Magnetic Properties of Nitronyl Nitroxide Triradicals Composed of Ground-State Singlet Biradicals and Monoradicals: Molecular Spin Clusters in the Crystal

Tomoaki Ise,[†,‡] Daisuke Shiomi,*[,†,‡,§] Kazunobu Sato,[†] and Takeji Takui*[,†]

Departments of Materials Science and Chemistry, Graduate School of Science, Osaka City University, Sumiyoshi-ku, Osaka 558-8585, Japan, and PRESTO, Japan Science and Technology Agency (JST), 4-1-8 Honcho Kawaguchi, Saitama 332-0012, Japan

Received March 12, 2005

We report X-ray crystal structures and magnetic properties of novel nitronyl nitroxide triradicals, *p*-triNN (**1**) and *m*-triNN (**2**), in which a ground-state singlet ($S = 0$) biradical with a π-conjugated phenol substituent and an $S = {}^1/_2$ carboxyl-substituted monoradicals are united by σ-bonds of an ester bridge. It is found for both **1** and **2** that the exchange interactions $J(\sigma)$ between the biradical and the monoradical moieties through the σ-bonds of the ester bridge are much smaller than those through the π-conjugation, $J(\pi)$, within the biradical moieties. Thus, the inequivalent magnetic degrees of freedom, one from the biradical and the other from the monoradical moiety, are retained in a single molecule. X-ray crystallography and magnetic susceptibility of **1** indicate that an intermolecular antiferromagnetic exchange interaction between the biradical and the monoradical moieties gives a three-spin cluster. On the other hand, the triradical **2** is found to form a six-spin cluster, consisting of two sets of monoradical−biradical pairs in the crystal. The formation of the molecular spin clusters in **1** and **2** gives us the way of developing exotic spin coupling systems from σ-bonded π-oligoradicals carrying multiple magnetic degrees of freedom.

Introduction

Over the past few decades, a considerable number of studies have been conducted on the molecule-based magnetic materials[1] since the discovery of the β-phase of *p*-NPNN,[2] the first example of a genuinely organic free radical with a bulk ferromagnetic transition. Much work has been devoted to the design of building blocks of new free radical derivatives such as nitronyl nitroxide for achieving exotic molecular magnetic materials.[1] Molecular packing, or relative arrangement of open-shell molecules, in a crystalline solid state has a crucial relationship with magnetic properties of molecular assemblages. Thus, the control of crystal structure or molecular packing in the molecule-based materials is one of the most important issues in the development of molecule-based magnetics. Noncovalent bonding such as hydrogen bonding[3] has been invoked to control the molecular packing of the open-shell molecules.

Covalent bonding can be another structure-determining binding force between open-shell entities for controlling molecular packing in organic molecular crystals as well as the noncovalent bondings. When two kinds of π-radicals with their unpaired electrons in π-orbitals are united by σ-bonds, π-conjugation in the resultant oligoradical is truncated at the σ-bond, giving rise to multiple magnetic degrees of freedom in a single molecule. A successful application of the covalently bonded open-shell entities has been found in ferrimagnetic spin alignment in the crystal of a nitronyl nitroxide triradical, in which a biradical in a triplet ($S = 1$) ground state and a monoradical with $S = {}^1/_2$ are united by σ-bonds of an ester bridge.[4] The ferrimagnetic spin alignment, i.e., an antiparallel coupling of $S = 1$ and $S = {}^1/_2$ spins, has been achieved by intermolecular π-orbital overlaps

* Authors to whom correspondence should be addressed. E-mail: shiomi@sci.osaka-cu.ac.jp; takui@sci.osaka-cu.ac.jp.

[†] Osaka City University.

[‡] Japan Science and Tecnology Agency.

[§] Address for Professor Daisuke Shiomi: Department of Materials Science, Graduate School of Science, Osaka City University, Sumiyoshi-ku, Osaka 558-8585, Japan. Tel: +81-6-6605-3149. Fax: +81-6-6605-3137.

(1) For reviews of molecule-based magnetics, see (a) Gatteschi, D., Kahn, O., Miller, J. S., Palacio, F., Eds. *Molecular Magnetic Materials*; KIuwer Academic: Dordrecht, 1991. (b) Iwamura, H.; Miller, J. S. *Mol. Cryst. Liq. Cryst.* **1993**, *232*, *233*. (c) Miller, J. S.; Epstein, A. J. *Mol. Cryst. Liq. Cryst.* **1995**, *271*−*274*. (d) Itoh, K.; Miller, J. S.; Takui, T. *Mol. Cryst. Liq. Cryst.* **1997**, *305*, *306*. (e) Kahn, O. *Mol. Cryst. Liq. Cryst.* **1999**, *334*, *335*. (f) Christou, G. *Polyhedron* **2001**, *20*. (g) Christou, G. *Polyhedron* **2003**, *22*. (h) Lahti, P, M., Ed. *Magnetic Properties of Organic Materials*; Marcel Dekker: New York, 1999. (i) Itoh, K., Kinoshita, M., Eds. *Molecular Magnetism: New Magnetic Materials*; Gordon & Breach: Amsterdam (Kodansha as copublisher, Tokyo), 2000.

(2) (a) Tamura, M.; Nakazawa, Y.; Shiomi, D.; Nozawa, K.; Hosokoshi, Y.; Ishikawa, M.; Takahashi, M.; Kinoshita, M. *Chem. Phys. Lett.* **1991**, *186*, 401. (b) Nakazawa, Y.; Tamura, M.; Shirakawa, N.; Shiomi, D.; Takahashi, M.; Kinoshita, M.; Ishikawa, M. *Phys. Rev. B* **1992**, *46* 8906.

(3) For example, see: (a) Cirujeda, J.; Ochando, L. E.; Amigo, J. M.; Rovira, C.; Rius, J.; Veciana, J. *Angew. Chem., Int. Ed. Eng.* **1995**, *34*, 55. (b) Cirujeda, J.; Mas, M.; Molins, E.; Panthou, F. L.; Laugien, J.; Park, J. G.; Paulsen, C.; Rey, P.; Rovira, C.; Veciana, J. *J. Chem. Soc., Chem. Commun.* **1995**, 709. (c) Veciana, J.; Cirujeda, J.; Rovira, C.; Molins, E.; Novoa, J. J. *J. Phys. I* **1996**, *6*, 1967. (d) Matsushita, M. M.; Izuoka, A.; Sugawara, T.; Kobayashi, T.; Wada, N.; Takeda, N.; Ishikawa, M. *J. Am. Chem. Soc.* **1997**, *119*, 4369. (e) Nagashima, H.; Yoshioka, N.; Inoue, H. *Polyhedron* **2001**, *20*, 1151. (f) Otsuka, T.; Okuno, T.; Awaga, K.; Inabe, T. *J. Mater. Chem.* **1998**, *8*, 1157. (g) Lahti, P. M.; Ferrer, J. R.; George, C.; Oliete, P.; Julier, M.; Palacio, F. *Polyhedron* **2001**, *20*, 1465.

(4) (a) Shiomi, D.; Kanaya, T.; Sato, K.; Mito, M.; Takeda, K.; Takui, T. *J. Am. Chem. Soc.* **2001**, *123*, 11823. (b) Kanaya, T.; Shiomi, D.; Sato, K.; Takui, T. *Polyhedron* **2001**, *20*, 1397. (c) Shiomi, D.; Nishizawa, M.; Kamiyama, K.;. Hase, S.; Kanaya, T.; Sato, K.; Takui, T. *Synth. Met.* **2001**, *121*, 1810. (d) Kaneda, C.; Shiomi, D.; Sato, K.; Takui, T. *Polyhedron* **2003**, *22*, 1809.

10.1021/cm050558b CCC: $30.25
Published on Web 07/22/2005

between an $S = 1$ moiety of one molecule and an $S = {}^1/_2$ moiety of the adjacent molecule, mimicking molecular complexation of π-biradicals and π-monoradicals. The σ-bonds in the triradical are magnetically inactive as a magnetic interaction pathway and play a role in the structural framework, while the magnetic interactions are propagated by the through-space π-orbital overlaps between the molecular entities of the adjacent molecules in the crystalline solid.

In this study, we extend the molecular design of σ-bonded oligoradicals to the case of a constituent biradical with a singlet ($S = 0$) ground state. The exchange coupling in the composite molecule composed of a ground-state singlet biradical and a doublet monoradical is described by a Heisenberg spin Hamiltonian

$$H = -2J(\sigma)\mathbf{S}_{b1}\cdot\mathbf{S}_m - 2J'(\sigma)\mathbf{S}_{b2}\cdot\mathbf{S}_m - 2J(\pi)\mathbf{S}_{b1}\cdot\mathbf{S}_{b2} \quad (1)$$

where the two $S = {}^1/_2$ spins, $\mathbf{S}_{b1}$ and $\mathbf{S}_{b2}$, are coupled by the antiferromagnetic exchange interaction $J(\pi) < 0$ through the π-conjugation in the biradical moiety and they are coupled with another $S = {}^1/_2$ spin, $\mathbf{S}_m$, in the monoradical moiety by the exchange interactions $J'(\sigma)$ and $J(\sigma)$ through the σ-bonds. In this phenomenological coupling scheme, the requisite for the magnetically inactive σ-bonds is represented by

$$|J(\sigma)|,|J'(\sigma)| \ll |J(\pi)| \quad (2)$$

If the magnetic interactions $J(\sigma)$ and $J'(\sigma)$ through the covalent bonds are in the same order of magnitude as $J(\pi)$ in the biradical moiety, the resultant triradical acts as merely a quartet ($S = {}^3/_2$) or a doublet ($S = {}^1/_2$) radical, depending on the sign of the additional interactions through the σ-bonds. We have designed and synthesized novel nitronyl nitroxide triradicals, *p*-triNN (4-(1′-oxyl-3′-oxido-4′,4′,5′,5′-tetramethyl-imidazolin-2′-yl)-benzoic acid 2,5-bis-(1″-oxyl-3″-oxido-4″,4″,5″,5″-tetramethyl-imidazolin-2″-yl)-phenyl ester; **1**) and *m*-triNN (3-(1′-oxyl-3′-oxido-4′,4′,5′,5′-tetramethyl-imidazolidin-2′-yl)-benzoic acid 2,5-bis-(1″-oxyl-3″-oxido-4″,4″,5″,5″-tetramethyl-imidazolidin-2″-yl)-phenyl ester; **2**), possessing a *para*-phenylene type biradical moiety with a singlet ground state and a monoradical moiety, as depicted in Chart 1.

The triradical compounds **1** and **2** were synthesized by esterification of a phenolic biradical with a singlet ground state **3**[5] and *para*- or *meta*-carboxyl-substituted monoradicals.[6,7] The parent biradical **3** is known to have a singlet ($S = 0$) ground state with the singlet−triplet energy gap of $2J(\pi)/k_B = -82$ K.[5] It is expected that the π-conjugation in the *p*-phenylene biradical moieties in **1** and **2** is truncated at the σ-bonds of the ester bridge. In fact, it has been known from our previous studies that the condition eq 2 is realized for $|J(\pi)|$ larger than $|J(\sigma)|$ and $|J'(\sigma)|$ by 3 orders of magnitude in **1**; $2|J(\sigma)|/k_B \sim 2|J'(\sigma)|/k_B \leq 0.01$ K.[5] In the present study, the amplitude of the intramolecular exchange interactions is examined for the triradical **2** and the condition eq 2 is verified for **2** as well as **1**. Temperature dependence of magnetic susceptibility of **1** and **2** measured for crystalline solids states is analyzed on the basis of their crystal structures, from which formation of exchange-coupled spin clusters are found in the crystals for both **1** and **2**.

Chart 1. Triradicals *p*-triNN (1) and *m*-triNN (2) and the Schematic Drawing of the Three-Centered Exchange Coupled System ($S_{b1} = S_{b2} = S_m = {}^1/_2$)[a]

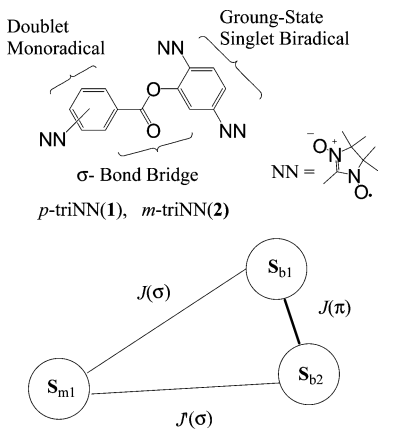

[a] $J(\sigma)$ and $J'(\sigma)$ show the weak interactions through the σ-bonds in **1** and **2**, while $J(\pi)$ denotes the antiferromagnetic interaction through the π-conjugation of the *para*-phenylene-based biradical moiety.

Scheme 1. Synthesis of *p*-triNN(1) and *m*-triNN(2)

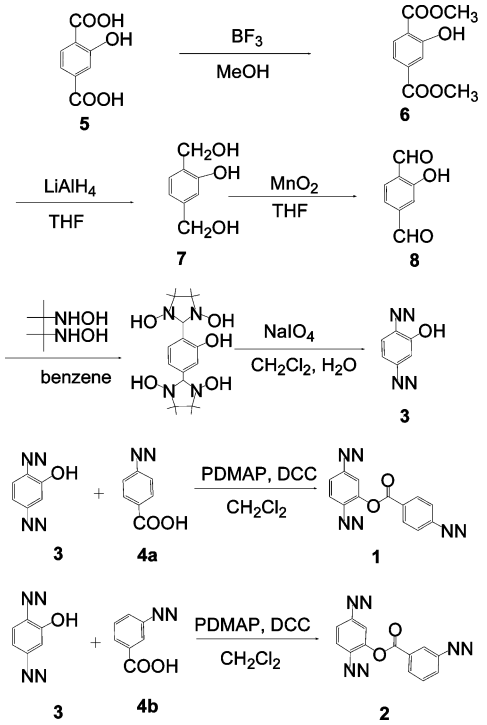

Experimental Section

Synthesis. Triradicals **1** and **2** were synthesized by esterification of the biradical **3**[5] and the monoradicals **4a**[6] and **4b**,[7] respectively, as shown in Scheme 1. Detailed synthetic procedures in Scheme 1 is provided as Supporting Information. The monoradicals **4a** and **4b** were synthesized according to literature procedures.[6,7]

p-triNN (1). A mixture of **3** (315 mg, 0.78 mmol), **4a** (270 mg, 0.98 mmol), and 4-(dimethylamino)pyridine (95 mg, 0.78 mmol) were dissolved in dry CH_2Cl_2 (35 mL) at 0 °C under an argon atmosphere. After the addition of *N*,*N*′-dicyclohexylcarbodiimide

(5) Ise, T.; Shiomi, D.; Sato, K.; Takui, T. *Synth. Met.*, in press.
(6) Inoue, K.; Iwamura, H. *Chem. Phys. Lett.* **1993**, *207*, 551.
(7) Schatzschneider, U.; Weyhermueller, T.; Rentschler, E. *Inorg. Chim. Acta* **2002**, *337*, 122.

(480 mg, 2.3 mmol) to the mixture solution, the reaction mixture was stirred for 4 h. After filtration, reaction solution was washed with aqueous HCl (0.5 M) and then the mixture solution was neutralized with aqueous $NaHCO_3$. The aqueous phase was extracted with CH_2Cl_2 (100 mL). The combined organic phase was dried over $MgSO_4$. The solution was concentrated and chromatographed over a silica gel column. Elution with CH_2Cl_2/acetone (8/1 in volume) followed by removal of the solvent in vacuo gave a pure blue product of 380 mg (73%). Elemental analysis (C, H, N) of *p*-triNN (**3**): Anal. Calcd for *p*-triNN·$^1/_2H_2O$: C, 60.70; H, 12.49; N, 6.59%. Found: C, 60.75; H, 12.40; N, 6.54%. Single crystals of **1** suitable for X-ray crystallography experiments were obtained by recrystallization from a mixture of acetone and hexane.

m-triNN (2). The triradical **2** was synthesized in the same way as that of **1**. Elemental analysis (C, H, N) of *m*-triNN (**2**): Anal. Calcd for *m*-triNN·H_2O·acetone: C, 60.07; H, 6.95; N, 11.36%. Found: C, 59.68; H, 6.83; N, 11.46%. Single crystals of **2** were obtained by diffusion of methanol into an acetone solution of **2**.

X-ray Crystallographic Analysis. Single-crystal diffraction data of **1** and **2** were collected on a Rigaku Mercury CCD diffractometer with graphite monochromated Mo Kα radiation at 105 and 143 K, respectively. The crystal structures were solved by using direct methods (SIR92) in a program package *CrystalStructure*.[8] Anisotropic temperature factors were applied for non-hydrogen atoms. Hydrogen atoms with isotropic thermal parameters were refined as riding models. CCDC reference numbers for *p*-triNN (**1**) and *m*-triNN (**2**) are 249575 and 249576, respectively.

Magnetic Susceptibility Measurements. Magnetic susceptibility was measured on a Quantum Design SQUID magnetometer MPMS-XL in the temperature range down to 1.9 K with a static field of 0.1 T. The magnetic responses were corrected with diamagnetic blank data of the sample holder obtained separately. The diamagnetic contribution of the sample itself was estimated from Pascal's constants. A PVC (poly(vinyl chloride)) film was prepared by slow evaporation of a CH_2Cl_2 solution of PVC and **2**, which was used as magnetically diluted samples.

Results and Discussion

1. X-ray Crystal Structures. The molecular structures and crystallographic parameters of *p*-triNN (**1**) and *m*-triNN (**2**) are given in Figure 1 and Table 1,[9] are quite similar as listed in Table 2 and Table 3. In contrast, the dihedral angles between the nitronyl nitroxide plane and the phenyl plane, and the intramolecular torsion angles between the two phenyl groups through the ester bridge, are considerably different. This is probably due to a difference in steric repulsion between the monoradical and the biradical moieties.

As shown in Figure 2a, the molecules of **1** are arranged in a head-to-tail fashion along the *a* axis. A short intermolecular distance of 3.294(6) Å is found between the nitroxide oxygen atom (O2) of the monoradical moiety and the nitrogen atom (N6*i*) of the biradical moiety of the neighboring, inversion-related molecule, where *i* denotes the symmetry operation of $-x + 1, -y, -z + 2$. This contact leads to a SOMO−SOMO (SOMO: singly occupied molecular orbital) overlap between the molecules and a sizable antiferromagnetic interaction is expected. No other intermolecular short distances close to the van der Waals contact[10] were found around the nitroxide groups with large spin density. These results indicate that the magnetic coupling in the

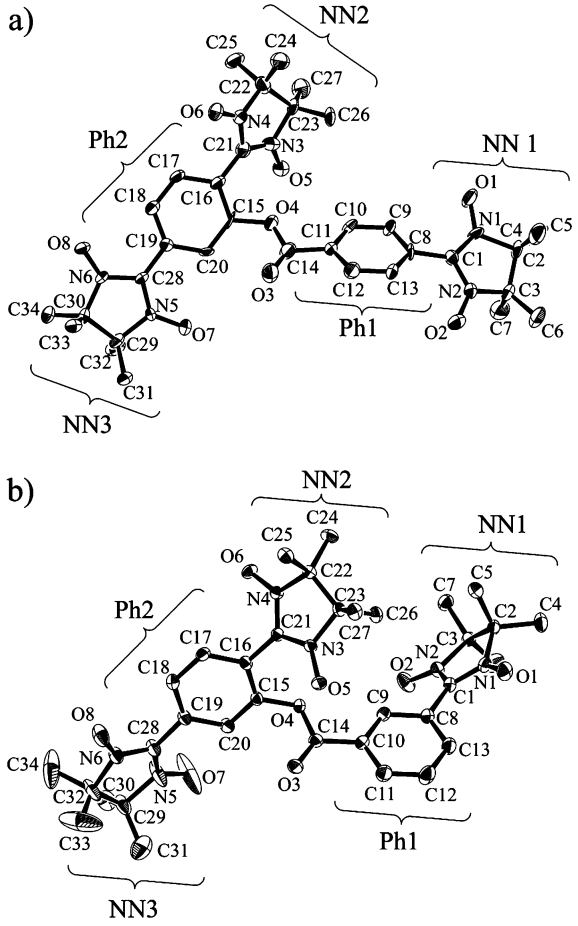

Figure 1. ORTEP views of the triradical molecules (a) *p*-triNN (**1**) and (b) *m*-triNN **(2)** at the 50% probability level. The hydrogen atoms in **1** and **2** are omitted for the sake of clarity.

Table 1. X-ray Crystallographic Data of *p*-triNN (1) and *m*-triNN (2)

compound	*p*-triNN (**1**)	*m*-triNN (**2**)
Formula	$C_{34}H_{43}N_6O_8$	$C_{37}H_{51}N_6O_{10}$ ($C_{34}H_{43}N_6O_8$·C_3H_6O·H_2O)
crystal system	triclinic	monoclinic
Space group	$P\bar{1}$	$P2_1/n$
a/Å	11.773(3)	17.6802(9)
b/Å	12.173(3)	10.3712 (4)
c/Å	14.493(2)	21.565(1)
α/deg	62.95(5)	
β/deg	67.76(5)	96.092(3)
γ/deg	70.49(5)	
V/Å^3	1678.9(6)	3931.9(3)
Z	2	4
D_{calc}/g cm^{-3}	1.313	1.250
T/K	105	143
unique reflections used ($I > 3\sigma(I)$)	5167	6055
$R_1(I > 3\sigma(I))^{a)}$	0.105	0.064
R_w(all data)$^{b)}$	0.217	0.199
goodness of fit	1.070	0.999

^{a} $R = \sum||F_o| - |F_c||/\sum|F_o|$. ^{b} $Rw = [\sum w(|F_o| - |F_c|)^2/\sum w(F_c)^2)]^{1/2}$; $w = 1/[0.0010F_o^2 + 3.0000\sigma(F_o^2) + 0.5000]/(4F_o^2)$.

(8) *Crystal Structure* (ver.3.6.0). Rigaku/Molecular Structure Corporation 9009 New Trails Dr., The Woodlands, TX 77381, USA, 2000−2004.

(9) The R_1 value of 0.105 for **1** results from disordered oxygen atoms of water. On the final difference Fourier map, density peaks with the maximum and minimum of 0.65 and −0.52 e/Å^3 were found, which were attributable to the disordered oxygen atoms. The refinement including the residual peaks was unsuccessful, resulting in difficulty of the least-squares calculation.

(10) Bondi, A. *J. Phys. Chem.* **1964**, *68*, 441.

Table 2. Selected Bond Distances (Å) for 1 and 2

	p-triNN (**1**)	*m*-triNN (**2**)
N1−O1	1.283(5)	1.279(3)
N2−O2	1.279(9)	1.291(2)
C1−N1	1.370(1)	1.345(3)
C1−N2	1.314(7)	1.338(3)
C1−C8	1.460(1)	1.464(3)
O5−N3	1.284(6)	1.278(2)
O6−N4	1.297(6)	1.287(2)
C21−N3	1.362(7)	1.349(3)
C21−N4	1.343(8)	1.342(3)
C21−C16	1.450(8)	1.464(3)
O8−N6	1.281(7)	1.276(3)
O7−N5	1.307(8)	1.281(5)
C28−N5	1.331(8)	1.328(4)
C28−N6	1.372(9)	1.348(3)
C28−C19	1.426(7)	1.464(3)

Table 3. Selected Bond Angles (deg) and Dihedral Angles[a] for 1 and 2

	p-triNN(**1**)	*m*-triNN(**2**)
N1−C1−N2	108.8(7)	109.4(2)
C1−N1−O1	128.7(6)	126.3(2)
C1−N2−O2	127.1(7)	125.8(2)
C1−N1−C3	110.2(4)	111.4(2)
C1−N2−C2	112.0(6)	112.1(2)
N3−C21−N4	107.4(5)	109.0(2)
C21−N3−O5	125.5(4)	125.8(2)
C21−N4−O6	124.8(4)	125.5(2)
C21−N3−C23	112.6(5)	111.9(2)
C21−N4−C22	112.2(4)	112.4(2)
N5−C28−N6	106.3(4)	108.9(2)
C28−N5−O7	125.1(5)	124.9(3)
C28−N6−O8	125.8(4)	126.1(2)
C28−N5−C29	115.4(6)	113.8(2)
C28−N6−C30	112.6(5)	113.2(2)
Ph1−Ph2	50.6(2)	69.6 (1)
NN1−Ph1	33.9(2)	40.3(2)
NN2−Ph2	53.1(2)	50.3(1)
NN3−Ph2	16.2(2)	28.4(1)

[a] Atoms defining the least-squared planes are as follows: O1−N1−C1−N2−O2 (NN1), O5−N3−C21−N4−O6 (NN2), O7−N5−C28−N6−O8 (NN3), C8−C9−C10−C11−C12−C13 (Ph1), and C15−C16−C17−C18−C19−C20 (Ph2).

crystal for **1** is approximated by a magnetically isolated six-spin system of the head-to-tail dimer, as depicted in Figure 2b.

In the crystal of **2**, two types of symmetry operations give rise to intermolecular short contacts around the nitroxide groups. One of the short contacts is found between the oxygen atom (O8) in the biradical moiety and the nitronyl nitroxide groups of the monoradical moiety neighboring along the [011] direction with the *n*-glide plane (the symmetry operation *n*: $x - {}^1/_2, -y + {}^1/_2, z - {}^1/_2$), 3.141(3) Å at O8−N1*n*, and 3.152(3) Å at O8−C1*n*, as depicted in Figure 3a. The other short contact is found at O5−N3*i* (3.529(2) Å) between the nitroxide groups of the inversion-related molecules (*i*: $-x, -y, -z + 2$), as shown in Figure 3b. These two types of intermolecular short contacts lead to a doubled chain structure of the triradical molecules running along the [011] direction, as depicted in Figure 3c. The magnetic coupling in the doubled chain is schematically shown in Figure 3d. The intermolecular exchange interaction originating from the contacts at O8−N1*n* and O8−C1*n* is labeled J_{2n}, while that from O5−N3*i* is designated as J_{2i}.

2. Magnetic Properties. *(a) p-triNN (1).* The temperature dependence of magnetic susceptibility χ_m for the polycrystalline sample of **1** is shown in Figure 4 in the $\chi_m T$ vs T

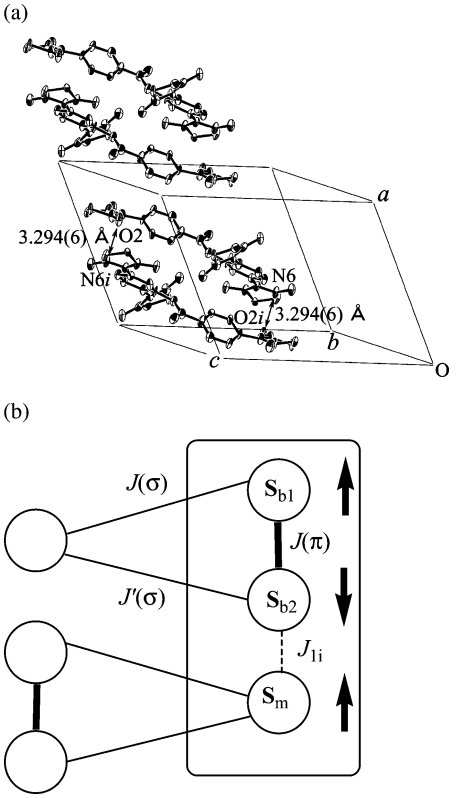

Figure 2. (a) Crystal structure of *p*-triNN (**1**) projected onto the *ac* plane. A short intermolecular distance of 3.294(6) Å is found between O2 and N6*i* of the inversion-related molecules (symmetry operation *i*: $-x + 1, -y, -z + 2$). The methyl groups and the hydrogen atoms are omitted for clarity. (b) Schematic diagram of the exchange coupling in the head-to-tail dimer of **1**. The circles denote the $S = {}^1/_2$ spins, which are coupled by the intramolecular exchange interactions $J(\pi)$, $J(\sigma)$, and $J'(\sigma)$. The intermolecular interaction at O2 and N6*i* is designated J_{1i}. The rounded rectangle represents the three-spin system of eq 3, which is used in the analysis of the magnetic susceptibility. The arrows indicate the spin alignment in the ground state.

plots. The $\chi_m T$ value of 1.1 emu mol^{-1} K at room temperature corresponds to 3 mol of $S = {}^1/_2$ spins. Upon cooling, the $\chi_m T$ value decreases and reaches a constant value of 0.39 emu mol^{-1} K below 10 K. The intramolecular exchange interaction $J(\sigma)$ and $J'(\sigma)$ through the ester bridge in **1** has been found to be $2|J(\sigma)|/k_B \sim 2|J'(\sigma)|/k_B \leq 0.01$ K[5] from magnetic susceptibility measurements for the sample dispersed in a polymer film of PVC (poly(vinyl chloride)), in which intermolecular magnetic interactions are suppressed. When $J(\sigma)$ and $J'(\sigma)$ are neglected, the six-spin system of the head-to-tail dimer of **1** (Figure 2b) deduced from the structural analysis is reduced to a three-spin system, which is represented by the three-centered Heisenberg spin Hamiltonian

$$H = -2J_{1i}\mathbf{S}_m\cdot\mathbf{S}_{b2} - 2J(\pi)\mathbf{S}_{b1}\cdot\mathbf{S}_{b2} \quad (3)$$

The exchange interaction J_{1i} corresponds to the intermolecular short contact at O2−N6*i*. The temperature dependence of $\chi_m T$ is analyzed using eq 4

$$\chi_m = \frac{\alpha N g^2 \mu_B{}^2}{4k_B T}\frac{10\exp[-E_Q/k_BT] + \exp[-E_{D1}/k_BT] + \exp[-E_{D2}/k_BT]}{2\exp[E_Q/k_BT] + \exp[-E_{D1}/k_BT] + \exp[-E_{D2}/k_BT]} \quad (4)$$

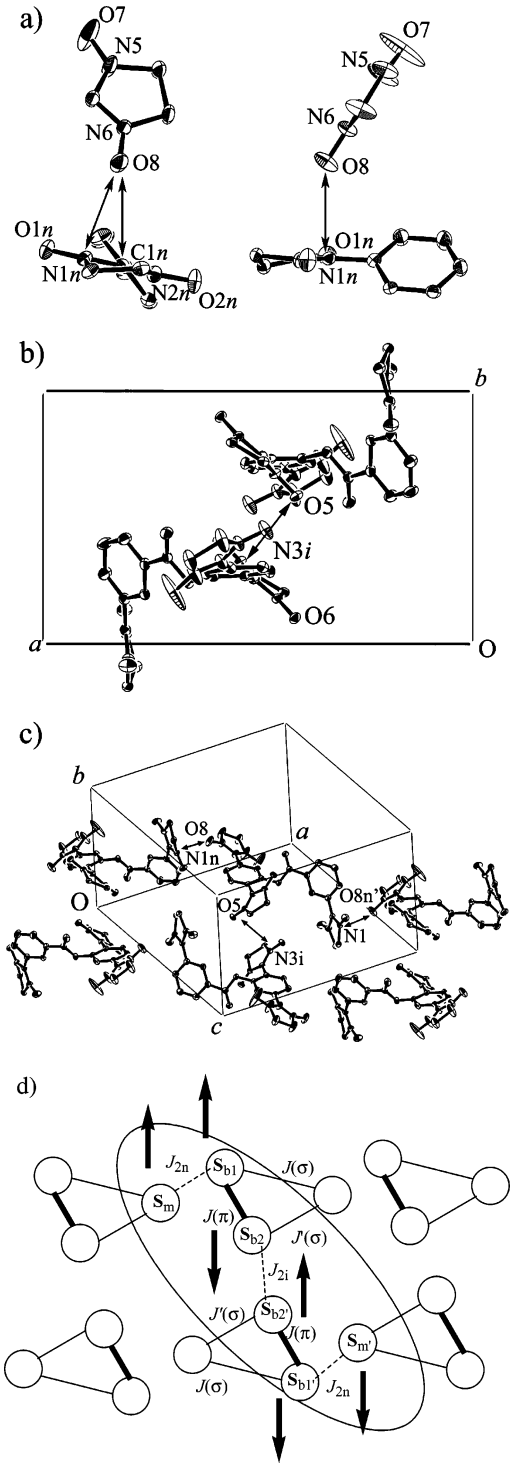

Figure 3. (a) Intermolecular short contacts of **2** between the neighboring molecules related by the *n*-glide plane (*n*: $x - {}^1/_2$, $-y + {}^1/_2$, $z - {}^1/_2$). Only the nitronyl nitroxide of the biradical entity and the phenyl group of the monoradical entity are shown. Intermolecular short contacts: 3.141(3) Å at O8−N1*n*, 3.152(3) Å at O8−C1*n*. (b) Intermolecular short contacts of **2** between the neighboring molecules related by the inversion center (*i*: $-x$, $-y$, $-z + 2$). Intermolecular short contacts: 3.529(2) Å at O5−N3*i*. (c) Molecular packing of **2** viewed along the *b* axis (*n*′: $x + {}^1/_2$, $-y + {}^1/_2$, $z + {}^1/_2$). The methyl groups and the hydrogen atoms in **2**, as well as the solvent molecules of acetone and water, are omitted for the sake of clarity. (d) Schematic diagram of the exchange coupling in the doubled chain of **2**. The circles denote the $S = {}^1/_2$ spins, which are coupled by the intramolecular exchange interactions $J(\pi)$, $J(\sigma)$, and $J'(\sigma)$. The intermolecular interaction at O8−N1*n* and O8−C1*n* is designated as J_{2n} and that at O5−N3*i* is J_{2i}. The oval represents the six-spin system of eq 8. The arrows indicate the spin alignment in the ground state.

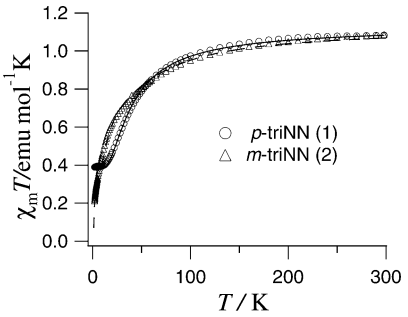

Figure 4. Temperature dependence of the product $\chi_m T$ measured at 0.1 T for **1** (circles) and **2** (triangles). The solid and dashed lines represent the theoretical calculations based on eq 3 and eq 8, respectively.

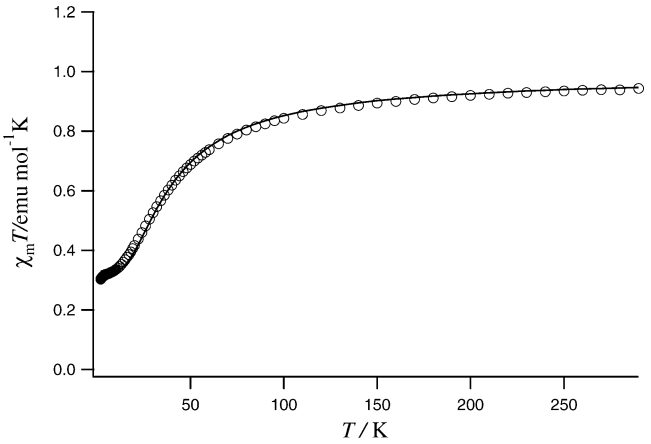

Figure 5. Temperature dependence of paramagnetic susceptibility χ_m of *m*-triNN (**2**) diluted in the PVC film in the $\chi_m T$ vs T plots. The solid line represents the theoretical calculation from eq 1.

where E_Q, E_{D1}, and E_{D2} denote the energy eigenvalues of eq 3 corresponding to a quartet ($S = {}^3/_2$) and two doublet ($S = {}^1/_2$) states, respectively:

$$E_Q = -\frac{1}{2}[J(\pi) + J_{1i}] \tag{5a}$$

$$E_{D1} = \frac{1}{2}[J(\pi) + J_{1i}] + \sqrt{J(\pi)^2 - J_{1i}J(\pi) + J_{1i}^2} \tag{5b}$$

$$E_{D2} = \frac{1}{2}[J(\pi) + J_{1i}] - \sqrt{J(\pi)^2 - J_{1i}J(\pi) + J_{1i}^2} \tag{5c}$$

The parameter α in eq 4 denotes the purity of the sample. The symbols N_A, g, μ_B, and k_B in eq 4 stand for Avogadro constant, the g-factor, Bohr magneton, and Boltzmann constant, respectively. The best fit parameters reproducing the observed temperature dependence of $\chi_m T$ are $2J_{1i}/k_B = -4.4 \pm 0.5$ K and $\alpha = 1.00$, as the fitting depicted by solid lines in Figure 5. The intramolecular interaction $J(\pi)$ was fixed as $2J(\pi)/k_B = -70$ K, which has been determined in the susceptibility measurements on the diluted samples.[5,11] The g-factor was also fixed as $g = 2.006$, which has been obtained from an ESR spectrum in a toluene solution at room temperature.[5]

(11) It is plausible that the intramolecular interaction $J(\pi)$ in the crystalline solid state is different from that in the PVC film, which is due to a possible change in molecular conformation. The interaction $J(\pi)$ was, however, kept unchanged in the simulation with eq 3 and eq 8 in order to avoid overparametrization.

(b) m-triNN (2). The magnitude of the intramolecular exchange interaction of **2** between the monoradical and biradical moieties $J(\sigma)$ and $J'(\sigma)$ though the σ-bonds of the ester bridge was examined by paramagnetic susceptibility χ_m for the sample dispersed in a PVC film. As shown in Figure 5, the $\chi_m T$ value decreases on cooling and reaches a plateau of 0.36 emu mol^{-1} K, indicating the occurrence of antiferromagnetic interactions within the molecule and a doublet ($S = {}^1/_2$) ground state. The temperature dependence of $\chi_m T$ is analyzed using the three-centered exchange coupling model, eq 1, as schematically shown in Chart 1. The energy eigenvalues of eq 1 are

$$E_Q = -\frac{1}{2}[J(\pi) + J(\sigma) + J'(\sigma)] \rightarrow -\frac{1}{2}J(\pi) - J(\sigma) \quad (6a)$$

$$E_{D1} = \frac{1}{2}[J(\pi) + J(\sigma) + J'(\sigma)] + A \rightarrow \frac{3}{2}J(\pi) \quad (6b)$$

$$E_{D2} = \frac{1}{2}[J(\pi) + J(\sigma) + J'(\sigma)] - A \rightarrow -\frac{1}{2}J(\pi) + 2J(\sigma) \quad (6c)$$

$$A = \sqrt{J(\pi)^2 + J(\sigma)^2 + J'(\sigma)^2 - J(\pi)J(\sigma) - J(\pi)J'(\sigma) - J(\sigma)J'(\sigma)} \quad (6d)$$

where the amplitude of $J'(\sigma)$ is assumed to be equal to $J(\sigma)$ in order to avoid overparametrization:

$$J'(\sigma) \rightarrow J(\sigma) \quad (7)$$

The temperature dependence of $\chi_m T$ is calculated by substituting these energy eigenvalues in eq 4 and the best fit parameters $\alpha = 0.88$,[12] $2J(\pi)/k_B = -72 \pm 0.5$ K, and $2J(\sigma)/k_B = -0.01 \pm 0.01$ K reproduced the observed values, as depicted in Figure 5. This result indicates that the magnitude of $J(\sigma)$ is much smaller than that of $J(\pi)$, and the π-conjugation is efficiently truncated at the σ-bond bridge in **2** as well as in **1**.

The temperature dependence of magnetic susceptibility χ_m for the polycrystalline sample of **2** is shown in Figure 4 in the $\chi_m T$ vs T plots. The $\chi_m T$ value of 1.1 emu mol^{-1} K at room temperature is slightly lower than that expected for three $S = {}^1/_2$ spins. This indicates the occurrence of antiferromagnetic exchange interactions, which is responsible for the decrease in $\chi_m T$ upon lowering the temperature. It should be noted that the $\chi_m T$ value at low temperatures is lower than that for 1 mol of $S = {}^1/_2$ spin, 0.38 emu mol^{-1} K for $g = 2.0$. Passing across the $\chi_m T$ value expected for 1 mol of $S = {}^1/_2$ spin on lowering the temperature clearly indicates the nonmagnetic (diamagnetic) ground state of the molecular assemblage of **2** in the crystalline solid state. The six-spin system of **2** derived from the structural analysis (Figure 3d) is represented by the spin Hamiltonian

$$H = -2J_{2n}(\mathbf{S}_m \cdot \mathbf{S}_{b1} + \mathbf{S}_{m'} \cdot \mathbf{S}_{b1'}) - 2J(\pi)(\mathbf{S}_{b1} \cdot \mathbf{S}_{b2} + \mathbf{S}_{b1'} \cdot \mathbf{S}_{b2'}) - 2J_{2i}\mathbf{S}_{b2} \cdot \mathbf{S}_{b2'} \quad (8)$$

(12) The reduced purity of 0.88 is attributed to decomposition during the preparation of the PVC film by slow evaporation of the CH_2Cl_2 solution.

The Hamiltonian eq 8 was numerically diagonalized to give energy eigenvalues for a quartet and doublet states,[13] from which the temperature dependence of $\chi_m T$ was calculated with eq 4. The fitting to the experimental data of **2** gave the best-fit parameters of $2J_{2n}/k_B = +32 \pm 2$ K and $2J_{2i}/k_B = -112 \pm 8$ K. The intramolecular interaction of $2J(\pi)/k_B = -72$ K determined from the magnetically diluted system was assumed to remain unchanged.[11]

The exchange interactions with the signs of $J_{2n} > 0$, $J_{2i} < 0$, and $J(\pi) < 0$ afford the spin alignment of the ground state as depicted in Figure 3d. The total spin of the six-spin cluster is $S = 0$. The central, 2-positioned carbon atom of nitronyl nitroxide usually has a negative spin density. An intermolecular short contact between the negatively spin-polarized central carbon atom and the nitroxide oxygen with a large, positive spin density, such as O8−C1*n* in **2**, is expected to give rise to an intermolecular ferromagnetic interaction. Examples of the contact between the central carbon and the nitroxide oxygen contributing to intermolecular ferromagnetic interactions have been found in other nitronyl nitroxide crystals.[6,14,15] In the molecular packing of **2**, the O8−C1*n* contact is responsible for the ferromagnetic interaction of $2J_{2n}/k_B = +32$ K. The other contact of 3.147(2) Å at O8−N1*n*, adjacent to the O8−C1*n* contact, is expected to contribute to an antiferromagnetic interaction originating from a direct SOMO−SOMO overlap. If the exchange interaction J_{2n} is antiferromagnetic, the total spin of the six-spin cluster is $S = 0$ as well. Simulation of $\chi_m T$ vs T assuming negative J_{2n} values, however, failed to reproduce the observed temperature dependence of $\chi_m T$. This excludes the possibility of negative J_{2n}. The weak intramolecular interactions $J(\sigma)$ and $J'(\sigma)$ act as intercluster magnetic interactions in the molecular assemblage of **2**. The suppression of $J(\sigma)$ and $J'(\sigma)$ due to the σ-bonds affords the well-isolated spin clusters.

Conclusion

We have demonstrated the preparation and full characterization of *p*-triNN (**1**) and *m*-triNN (**2**), which possess both the monoradical and biradical entities united by the σ-bonds in the single molecule. From the magnetic susceptibility measurements and the crystal structure analyses, it has been found that the triradicals are assembled to form the molecular spin clusters in the crystalline solid states. Magnetic couplings between the spin clusters are undetectable for both **1** and **2** in the temperature range examined, indicating that the exchange interactions through the σ-bonds are well-suppressed.

The conceptual advance of the molecular designing for the σ-bonded π-oligoradicals lies in the fact that inequivalent

(13) The matrix dimension for the spin Hamiltonian eq 8 is $2^6 \times 2^6 = 64 \times 64$. The matrix was block-diagonalized according to conservation of the *z* component of the total spin, giving submatrices with the largest dimension of ${}_6C_3 \times {}_6C_3 = 20 \times 20$. The reduced dimension of the submatrix is still large, preventing analytical diagonalization like eq 1 and eq 3. Numerical diagonalization was applied to eq 8.

(14) Omata, J.; Ishida, T.; Hashizume, D.; Iwasaki, F.; Nogami, T. *Inorg. Chem.* **2001**, *40*, 3954.

(15) Panthou, F. L.; Luneau, D.; Laugier, J.; Rey, P. *J. Am. Chem. Soc.* **1993**, *115*, 9095.

magnetic entities such as π-biradicals and π-monoradicals are forced to coexist in a crystalline solid state. In this context, the fact enables us to construct exotic spin coupling systems in a crystalline solid state from σ-bonded π-oligoradicals with multiple magnetic degrees of freedom in a single molecule. One of the underlying motivations for the combination of ground-state singlet biradicals and monoradicals is to develop generalized ferrimagnetics[16] which have arisen from a close study of genuinely organic molecule-based magnetic materials. We have reported a theoretical prediction that an alternating chain system of ground-state singlet biradicals and doublet monoradicals has a ferrimagnetic-like high-spin ground state.[16] In nonquantum terms, biradicals with a singlet ($S = 0$) ground state would seemingly have no contribution to the magnetization at low temperatures. A quantum mechanical effect underlain by the magnetic degree of freedom within the ground-state singlet biradical affords a possibility of the ferrimagnetic-like high-spin ground state.[16] The formation of the molecular spin clusters in **1** and **2** gives us the way of developing the generalized ferrimagnet which needs both the forced cocrystallization of inequivalent molecules and retention of the magnetic degrees of freedom. Preparation of other σ-bonded triradicals composed of a ground-state singlet biradical and a monoradical as building blocks for the generalized ferrimagnets is currently underway.

Acknowledgment. This work has been supported by Grants-in-Aid for Scientific Research from the Ministry of Education, Sports, Culture, Science and Technology, Japan. Financial support from PRESTO of Japan Science and Technology Agency (JST) is also acknowledged. One of the authors (T. Ise) acknowledges JST postdoctoral fellowship.

Supporting Information Available: Synthetic procedures for compounds in Scheme 1 and crystallographic data (CIF files) for **1** and **2**. This material is available free of charge via the Internet at http:// pubs.acs.org.

CM050558B

(16) Shiomi, D.; Sato, K.; Takui, T. *J. Phys. Chem. B* **2001**, *105*, 2932.